TS-MPC for Autonomous Vehicles Including a TS-MHE-UIO Estimator

Eugenio Alcalá, Vicenç Puig, and Joseba Quevedo

***Abstract*—In this paper, a novel approach is presented to solve the trajectory tracking problem for autonomous vehicles. This approach is based on the use of a cascade control where the external loop solves the position control using a novel Takagi Sugeno-Model Predictive Control (TS-MPC) approach and the internal loop is in charge of the dynamic control of the vehicle using a Takagi Sugeno-Linear Quadratic Regulator technique designed via Linear Matrix Inequalities (TS-LMI-LQR). Both techniques use a TS representation of the kinematic and dynamic models of the vehicle. In addition, a novel Takagi–Sugeno estimator-Moving Horizon Estimator-Unknown Input Observer (TS-MHE-UIO) is presented. This method estimates the dynamic states of the vehicle optimally as well as the force of friction acting on the vehicle that is used to reduce the control efforts. The innovative contribution of the TS-MPC and TS-MHE-UIO techniques is that using the TS model formulation of the vehicle allows us to solve the nonlinear problem as if it were linear, reducing computation times by 10–20 times. To demonstrate the potential of the TS-MPC, we propose a comparison between three methods of solving the kinematic control problem: Using the nonlinear MPC formulation (NL-MPC) with compensated friction force, the TS-MPC approach with compensated friction force, and TS-MPC without compensated friction force.**

***Index Terms*—Autonomous vehicle, Takagi–Sugeno, MPC, MHE, UIO, LMI, state estimation.**

I. Introduction

In THE last recent years, we have experienced a great advance in the technological career towards autonomous driving. Today, we can see how research centers and large companies in the automotive sectors are accelerating and investing large amounts of money. In addition, if we add to this progress the advances in legislation and the increasing acceptance of the user, we converge on the fact that driving, as we know it today, has days counted. The numerous advantages that the autonomous vehicle offers with respect to traditional vehicles are obvious. However, the most attractive is the great reduction of accidents on the roads, which will lead to a huge reduction in deaths on roads worldwide.

Manuscript received May 23, 2018; revised October 29, 2018 and February 27, 2019; accepted May 16, 2019. Date of publication May 22, 2019; date of current version July 16, 2019. This work was supported by the Spanish Ministry of Economy and Competitiveness (MINECO) and FEDER through the Projects SCAV (ref. DPI2017-88403-R) and HARCRICS (ref. DPI2014-58104-R). The corresponding author, Eugenio Alcalá, is supported under FI AGAUR Grant (ref 2017 FI B00433). The review of this paper was coordinated by Dr. E. Velenis. *(Corresponding author: Eugenio Alcalá.)*

The authors are with the Department of Automatic Control, Polytechnic University of Catalonia, Barcelona 08034, Spain (e-mail: eugenio.alcala@upc.edu; vicenc.puig@upc.edu; joseba.quevedo@upc.edu).

In order to achieve complete autonomous driving, a series of modules are needed working in a sequential and organized manner. First, the vehicle sensing network (GPS, IMU, encoders, cameras, LIDAR, etc) collects all the vehicle and environment information and is treated to extract measurements of interest (vehicle position and obstacles around, inertial measures, etc). Then, the trajectory planning module is responsible for generating the route using the actual vehicle position and the desired one. This trajectory is composed of global positions, orientations and vehicle velocities. Finally, the automatic control which, using this sequence of references and the position of the vehicle, generates the control actions (acceleration, steering and braking) for the actuators.

The automatic control is the last piece in the sequence of the autonomous vehicle and one of the most important tasks since it is in charge of its movement. It is also the topic addressed in this paper. The control problem can be defined by two general features: the type of control (lateral, longitudinal or integrated) and the type of model considered for its design (kinematic, linear dynamic, simplified non-linear dynamics or non-linear dynamics). Articles [1] and [2] address the problem of lateral control using non-linear feedback control techniques. Optimal-based techniques like LQR for lateral control problem is formulated in [3]. Regarding the longitudinal control, we can find LQR strategy in [4], [5] and H_2 in [4]. However, these control strategies solve simplified versions of the real problem, i.e. the integrated control. This work addresses both the longitudinal-lateral integrated control problem for autonomous vehicles.

Control strategies based on Linear Parameter Varying (LPV) and Takagi Sugeno (TS) models are techniques for solving nonlinear problems using pseudo-linear models incorporating the non-linearities within the model parameters that depend on some scheduling variables. The recent books, [6], [7], [8], [9] and [10], presented the study of the modeling and design of LPV and TS under the formulation based on LMI. Several design approaches can be used such as pole positioning, $H\infty$, H_2 and LQR. These techniques have proven to be widely accepted in the field of robotics, for example [8] and [11].

Model Predictive Control (MPC) is another technique that has proven to be one of the most interesting methods in this field in recent years. This strategy allows to find the optimal control action through the resolution of a constrained optimization problem in which a mathematical model of the real system is evaluated in a future horizon. Recent articles such as [12], [13] and [14] present the latest advances in MPC control outside the automotive field. In the field of autonomous vehicles, we can

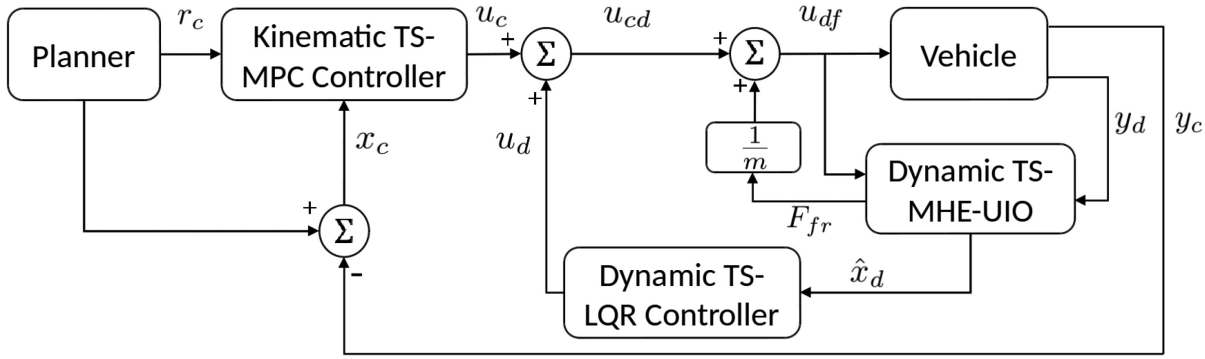

Fig. 1. Autonomous guidance diagram with kinematic and dynamic control layers and a dynamic state estimator with friction force compensator.

find all kinds of formulations for the MPC. From NLMPC applications in [15], where the lateral control problem is solved, to MPC lateral control using a linearized model of the vehicle in [16]. Working with nonlinear models give the best results. However, when working with systems with fast dynamics this technique may result non-viable since its excessive computational time. This is the reason why recent exploration of other ways opens the door to ideas such as mixing LPV-MPC or TS-MPC.

In [17], [18] present the MPC strategy using LPV models. In this work, we present the first TS-MPC formulation as an innovative control technique applied to the field of autonomous vehicles.

The advantage of TS and LPV approaches is that the nonlinear model can be expressed as a combination of linear models with parameter varying with some scheduling variables without using linearization [19].

The state measurement task will depend on the type of sensors installed on the vehicle and will be of vital importance for the application of certain control strategies. The longitudinal and angular speeds are magnitudes easy to measure using low cost sensors and are common in many of today's vehicles. On the other hand, there are other variables that are more complicated or expensive to measure. That is why the estimation of the system states is a problem of great interest in the automotive field.

Regarding the external disturbances, one of the magnitudes that disturb with greater impact the dynamics of the vehicle is the friction force. This one depends on the type of materials involved in the wheel-road contact. The rubber-asphalt contact is the most common and generates a magnitude of friction force that can be drastically altered if the vehicle suddenly crosses a wet or even frozen area. For this reason, the estimation and subsequent compensation of this force by the control strategy is of great interest in the field of autonomous driving. In recent years, different approaches have been addressed in the area of disturbance estimation for autonomous vehicles such as [20]–[23]. One of these techniques is the Unknown Input Observer (UIO). This approach has been widely used for detection and isolation of faults [24] and presented in the autonomous vehicle field [23]. This type of observer allows to estimate the states of a system, as well as the disturbances or uncertainty not modeled in the system.

The contribution of this paper is twofold and focuses on the use of Takagi Sugeno polytopic models for the design of the control and observation stages. First, the Model Predictive Control (MPC) technique is designed with a Takagi Sugeno (TS) kinematic model that leads to a quadratic problem. In addition, introducing the terminal set concept, we are able to guarantee stability.

Second, the Moving Horizon Estimator (MHE) strategy is merged with the use of a dynamic vehicle model formulated as Takagi Sugeno (TS) as well as with the Unknown Input Observer (UIO) concept, thus allowing the estimation of states and disturbances through a very fast predictive optimization (TS-MHE-UIO).

The paper is structured as follows: Section II gives an overview of the work and describes the different types of modelling used for control and estimation purposes. In Section III, the kinematic and dynamic control designs are developed. Section IV shows the TS-MHE-UIO design. Section V shows the simulation results and Section VI presents the conclusions of the work.

II. Overview of the Proposed Solution

We consider the problem of autonomous guidance of a vehicle in a racing scenario. To do so, two important tasks have to be carried out: the trajectory planning and the automatic control.

On one hand, the planning of the trajectory to be followed by the vehicle has to fulfill certain specifications such as continuous and differentiable velocity profiles. Thus, this module is in charge of providing discrete and smooth references to the automatic control stage. On the other hand, the automatic control is in charge of following the planned references, thus, moving the vehicle between two ground coordinates as well as generating smooth control actions for achieving a comfortable journey. In Fig. 1, we show the planning-control-estimation diagram proposed in this work. Observe that two control levels have been designed, one for the position control and the other one to control the dynamic behaviour of the vehicle, i.e. linear and angular velocities. In addition, the lack of measurement of certain vehicle states as well as the lack of knowledge of external disturbances can generate a problem when applying the designed control. Therefore, a dynamic estimator is introduced to solve this problem (see Fig. 1).

The level of difficulty of a vehicle guidance control problem comes often determined by two aspects: the type of control (lateral, longitudinal or mixed) and the complexity of the model to be controlled (kinematic, linear dynamic, non-linear simplified dynamic or non-linear dynamic). In this work we address one of the most complex configuration, the mixed non-linear dynamic problem. The following subsection covers the formulation of the different models used for solving the estimation and control problems.

A. Takagi-Sugeno Control Oriented Models

Unlike controlling common mobile robots which operate at a low interval of velocities and accelerations, racing cars work in a higher acceleration range. This fact makes indispensable to study control techniques based on elaborated dynamic models. Particularly with the aim of being safer and smoother in the control performance. In this work, two model-based techniques cover the kinematic and dynamic control and estimation. For that reason, the use of mathematical kinematic and dynamic vehicle models are necessary. The kinematic model is based on the mass-point assumption while for the dynamic one the bicycle model has been considered. We refer to the Appendix A for the complete model equations used in this paper.

In the following subsections, we present the TS formulation of both, the kinematic and dynamic models.

1) Kinematic TS Model: Denoting the state, control and reference vectors, respectively, as

$$x_c = \begin{bmatrix} x_e \\ y_e \\ \theta_e \end{bmatrix},\ u_c = \begin{bmatrix} v_x \\ \omega \end{bmatrix},\ r_c = \begin{bmatrix} v_d \cos\theta_e \\ \omega_d \end{bmatrix}, \tag{1a}$$

where x_e, y_e and θ_e are the position and orientation errors, respectively. The inputs v_x and ω are the longitudinal and angular velocities, respectively. v_d and ω_d are the longitudinal and angular reference velocities, respectively (see Fig. 2). Then, defining the vector of scheduling variables as $\rho(k) := [\omega(k), v_d(k), \theta_e(k)]$ which are bounded in $\omega \in [-3, 3]\ \frac{rad}{s}$, $v_d \in [0.1, 3.5]\ \frac{m}{s}$ and $\theta_e \in [-0.15, 0.15]\ rad$, the non-linear kinematic model (see Chapter 1 of [25]) is transformed into the Takagi-Sugeno representation by using the sector nonlinearity approach [6]

$$x_c(k+1) = A_c(\rho(k))x_c(k) + B_c u_c(k) - B_c r_c(k), \tag{1b}$$

where

$$A_c\left(\rho(k)\right) = \begin{bmatrix} 1 & \omega T_c & 0 \\ -\omega T_c & 1 & v_d \frac{\sin\theta_e}{\theta_e} T_c \\ 0 & 0 & 1 \end{bmatrix} \tag{1c}$$

$$B_c = \begin{bmatrix} -1 & 0 \\ 0 & 0 \\ 0 & -1 \end{bmatrix} T_c, \tag{1d}$$

with T_c being the kinematic sampling time.

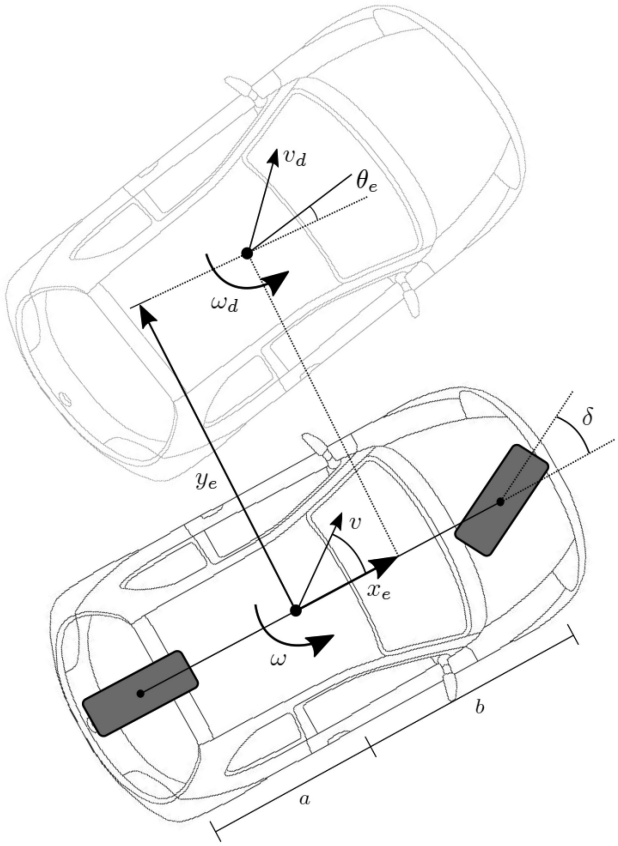

Fig. 2. Bicycle model used for estimation/control purposes. The vector v represents the velocity module. δ is the steering angle.

From this formulation, a polytopic representation for the control design is obtained as

$$x_c(k+1) = \sum_{i=1}^{2^{r_c}} \mu_i(\rho(k)) A_{c_i} x_c(k) + B_c u_c(k) - B_c r_c(k), \tag{2}$$

being r_c the number of scheduling variables and A_i each one of the polytopic vertex systems obtained as a combination of the extreme values of the scheduling variables.

The expression $\mu_i(\rho(k))$ is known as the membership function and is given by

$$\mu_i(\rho(k)) = \prod_{j=1}^{r_c} \xi_{ij}(\eta_0^j, \eta_1^j), \quad i = \{1, \ldots, 2^{r_c}\} \tag{3a}$$

$$\eta_0^j = \frac{\overline{\rho_j} - \rho_j(k)}{\overline{\rho_j} - \underline{\rho_j}}$$

$$\eta_1^j = 1 - \eta_0^j, \qquad j = \{1, \ldots, r_c\}, \tag{3b}$$

where $\xi_{ij}(\eta_0^j, \eta_1^j)$ corresponds to any of the weighting function that depend on each rule i.

2) Dynamic TS Model: The dynamic TS model considered in this work is a transformation of the non-linear one presented in [23].

Then, the state and control vectors are denoted as

$$x_d = \begin{bmatrix} v_x \\ v_y \\ \omega \end{bmatrix},\ u_d = \begin{bmatrix} \delta \\ a \end{bmatrix}, \tag{4a}$$

where v_y, a and δ are the lateral velocity, longitudinal acceleration and steering angle, respectively. Considering an unknown friction force disturbance F_{fr} as a variation of the nominal friction force ($\mu_o mg$). The Takagi-Sugeno model can be expressed as

$$x_d(k+1) = A_d(\vartheta(k))x_d(k) + B_d u_d(k) + E_d F_{fr}(k) \tag{4b}$$

where $\vartheta(k) := [\delta(k), v_x(k), v_y(k)]$ with $\delta \in [-0.35, 0.35]\ rad$, $v_x \in [0.1, 3.5]\ \frac{m}{s}$ and $v_y \in [-2, 2]\ \frac{m}{s}$; and

$$A_d(\vartheta(k)) = \begin{bmatrix} 1 + A_{11}T_d & A_{12}T_d & A_{13}T_d \\ 0 & 1 + A_{22}T_d & A_{23}T_d \\ 0 & A_{32}T_d & 1 + A_{33}T_d \end{bmatrix} \tag{4c}$$

$$A_{11} = -\frac{\mu_o g}{v_x},\ A_{12} = \frac{C_f \sin\delta}{m v_x} \tag{4d}$$

$$A_{13} = \frac{C_f l_f \sin\delta}{m v_x} + v_y,\ A_{22} = -\frac{C_r + C_f \cos\delta}{m v_x} \tag{4e}$$

$$A_{23} = -\frac{C_f l_f \cos\delta - C_r l_r}{m v_x} - v_x \tag{4f}$$

$$A_{32} = -\frac{C_f l_f \cos\delta - C_r l_r}{I v_x},\ A_{33} = -\frac{C_f l_f^2 \cos\delta + C_r l_r^2}{I v_x} \tag{4g}$$

$$B_d = \begin{bmatrix} 0 & 1 \\ B_{21} & 0 \\ B_{31} & 0 \end{bmatrix} T_d \tag{4h}$$

$$B_{21} = \frac{C_f}{m},\ B_{31} = \frac{C_f l_f}{I} \tag{4i}$$

$$E_d = \begin{bmatrix} \frac{-1}{m} \\ 0 \\ 0 \end{bmatrix} T_d, \tag{4j}$$

with T_d being the sample time using in the dynamic control. m and I represent the vehicle mass and inertia, respectively. l_f and l_r are the distances from the center of gravity to the front and rear wheel axes, respectively. Variables C_f and C_r represent the tire stiffness coefficient for the front and rear wheels. μ_o is the nominal friction coefficient.

As in the case of kinematic model, we look for a polytopic dynamic formulation like the following

$$x_d(k+1) = \sum_{i=1}^{2^{r_d}} \mu_i\big(\vartheta(k)\big) A_{d_i} x_d(k) + B_{d_i} u_d(k) + E_d F_{fr}(k), \tag{5}$$

being r_d the number of dynamic scheduling variables and A_{d_i} represent each one of the polytopic vertex dynamic systems obtained as a combination of the extreme values of the dynamic scheduling variables. The membership function is the same than the one presented in (2) but using the dynamic scheduling vector $\vartheta(k)$.

III. Control Design

In this section, we present the control scheme proposed for this work as well as its design. The control strategy of the vehicle has been divided into two nested layers, see Fig. 1. The outermost layer controls the vehicle's kinematics, i.e. its position and orientation, and works at a frequency of 20 Hz. On the other hand, the internal loop controls the dynamic behavior of the vehicle, i.e. its speeds, at a frequency of 200 Hz. Next, both control loops are described separately.

A. Kinematic TS-MPC Design

At this point, we present the formulation of the Takagi Sugeno Model Predictive Control strategy, which focuses on solving position and orientation control of the vehicle.

This strategy is based on the resolution of a linear quadratic optimization problem by using the non-linear kinematic error model in its TS polytopic representation. However, there exist the problem associated with the lack of knowledge of the matrix of scheduling variables through the entire prediction horizon. In [17], the use of the optimized state sequence which is obtained after each optimization is proposed.

In this work, the scheduling variables are states of the system whose desired values are known since the trajectory planner generates them. That is why we propose the use of such references as known scheduling variables for the entire optimization horizon being then the scheduling sequence $\Gamma := [\rho(k), \ldots, \rho(k+N)]$. In this way, we can calculate the evolution of the model more accurately and in anticipation.

In addition, since the basic MPC formulation cannot guarantee the overall stability of the system, we propose the addition of a terminal constraint and a terminal cost to the optimization problem.

To formulate the problem, the polytopic TS system presented in (2) has been considered. In order to avoid a difficult reading, the sub-index c is omitted in the rest of the subsection. Then, the focus is on a model predictive control scheme where the cost function is defined as

$$\mathrm{J_k} = \sum_{i=0}^{N-1} \left(x_{k+i}^T Q x_{k+i} + \Delta u_{k+i} R \Delta u_{k+i}\right) + x_{k+N}^T P x_{k+N}, \tag{6}$$

where $Q = Q^T \geq 0$, $R = R^T > 0$ and $P = P^T > 0$ represent the states, input and terminal set tuning, respectively.

At each time k the values of x_k and u_{k-1} are known and the following optimization problem can be solved

$$\underset{\Delta U_k}{\text{minimize}}\ \mathrm{J_k}(\Delta U_k, X_k)$$

subject to

$$\begin{aligned} & x_{k+i+1} = \sum_{j=1}^{2^{r_c}} \mu_j(\rho_{k+i}) A_j x_{k+i} + B u_{k+i} - B r_{k+i} \\ & u_{k+i} = u_{k+i-1} + \Delta u_{k+i} \qquad i = 0, \ldots, N-1 \\ & \Delta U_k \in \Delta\Pi \\ & U_k \in \Pi \\ & x_{k+N} \in \chi, \end{aligned} \tag{7}$$

where

$$\Delta U_k = \begin{bmatrix} \Delta u_k \\ \Delta u_{k+1} \\ \vdots \\ \Delta u_{k+N-1} \end{bmatrix} \in \mathbb{R}^m,\ U_k = \begin{bmatrix} u_k \\ u_{k+1} \\ \vdots \\ u_{k+N-1} \end{bmatrix} \in \mathbb{R}^m, \quad (8)$$

being m the number of inputs of the kinematic system. Π and $\Delta\Pi$ are the constraint sets for the inputs and their derivatives, respectively.

The set χ represents the terminal state domain. Then, by introducing this constraint in the optimization problem, we force the states to converge into a stable region and then, to ensure the MPC stability. The computation of this terminal set is carried out by solving two LMI-based problems.

First, the controller for each polytopic system (A_i) is found by solving the following LQR-LMI

$$\begin{bmatrix} Y & (A_iY + BW_i)^T & Y & W_i^T \\ A_iY + BW_i & Y & 0 & 0 \\ Y & 0 & Q_{TS}^{-1} & 0 \\ W_i & 0 & 0 & R_{TS}^{-1} \end{bmatrix} \geq 0$$
$$i = 1, \ldots, 2^{r_c}, \quad (9)$$

with $Y = Y^T > 0$, $Q_{TS} = Q_{TS}^T \geq 0$, $R_{TS} = R_{TS}^T > 0$. This problem returns the matrices Y and W_i. Then, the resulting controllers are obtained by $K_i = W_iY^{-1}$. Note that the terminal set matrix P in (6) is found to be equal to Y^{-1}.

This LQR design is a particular formulation for the one presented in Theorem 25 of [6]. The constant nature of kinematic input matrix B_c in (1) allows the use of this simplified LMI version.

The second problem consists on finding the largest terminal region χ. To do so, we solve the following constrained optimization problem using the previously obtained controllers K_i

$$\underset{Z}{\text{maximize}}\ \mathrm{J_k}(Z)$$
subject to
$$\begin{bmatrix} -Z & Z(A_i + BK_i)^T \\ (A_i + BK_i)Z & -Z \end{bmatrix} < 0$$
$$K_iZK_i^T - \overline{u}^2 < 0 \quad i = 1, \ldots, 2^{r_c}. \quad (10)$$

The resulting variable is Z. Hence, we compute the largest terminal region as $\chi = \{x | x^T S x \leq 1\}$, with $S = Z^{-1}$. Note that this problem is totally constrained by the maximum values of the control actions.

B. Dynamic TS-LQR Design

To design the dynamic controller we use the polytopic system (5). Then, we solve offline the optimal LMI problem (9) for computing the polytope vertex controllers K_i.

Finally, the dynamic controller gain is computed online following

$$K(\vartheta(k)) = \sum_{i=1}^{2^{r_d}} \mu_i(\vartheta(k))K_i, \quad (11)$$

where $\mu_i(\vartheta(k))$ represents the weighting function presented in (3) by using the dynamic scheduling vector defined in (4).

The offline computation of polytopic controllers allows this control strategy to work at the desired frequency of 200 Hz.

IV. TS-MHE-UIO Design

On one hand, the aim of the Moving Horizon Estimator is to predict the dynamic states for the next iteration by means of running a constrained optimization and using a set of past allowed measurements. Currently, it is usual to have experimental vehicles with different kind of sensors mounted on it that allows the measurement of almost every dynamic variable of the vehicle. However, most of the cheap versions of sensors are noisy and need of a post processing. Then, it is at this point where the state estimator gains interest.

The Unknown Input Observer approach deals with the estimation of external disturbances. One of the most relevant disturbances in road vehicles is the continuous change of road surface. This is why the coefficient of friction varies producing a remarkable alteration in the total computation of acting forces, drastically affecting the behavior of the vehicle.

In this section, we present a novel approach combining both the MHE and the UIO, to converge to an optimal state estimator able to predict disturbances. In addition, using a TS model formulation for computing the evolution during the established horizon allows the algorithm to run faster than non-linear model-based MHE.

To avoid a difficult reading, the sub-index d is omitted in system vectors but not in systems matrices.

A. UIO

The UIO goal is to estimate the main disturbances acting over the vehicle. Such a procedure is based on calculating the difference between the observation model and the real system [26]. In this work, we have considered as the disturbance the friction force acting in the longitudinal vehicle axis

$$F_{fr}(k) = \Theta\left(y(k) - C_d\left(\sum_{i=1}^{2^r} \mu_i(\vartheta_k)A_{d_i}\hat{x} + B_d u\right)\right), \quad (12)$$

with

$$C_d = \begin{bmatrix} 1 & 0 & 0 \\ 0 & 1 & 0 \\ 0 & 0 & 1 \end{bmatrix},\ \hat{x} = \begin{bmatrix} \hat{v_x} \\ \hat{v_y} \\ \hat{\omega} \end{bmatrix},\ \Theta = (C_dE_d)^+, \quad (13)$$

where A_{d_i}, B_d and E_d are the dynamic system matrices in (4) and $\mu_i(\vartheta_k)$ represents the weighting function presented in (3) by using the dynamic scheduling vector ϑ defined in (4).

Then, at every control iteration and once the state estimation has been solved, F_{fr} is computed.

B. TS-MHE Design

In order to design the MHE-UIO, the polytopic TS system (5) is used. In this work, it is considered that all the dynamic states (4a) are measured being then the filtering task the main work of the estimator.

The MHE optimization problem is based on minimizing the following cost function

$$\begin{aligned} \mathrm{J_k} &= (\hat{x}_{k-N} - x_o)^T P (\hat{x}_{k-N} - x_o) \\ &+ \sum_{i=-N}^{0} \left(w_{k+i}^T Q w_{k+i} + s_{k+i}^T R s_{k+i} \right), \end{aligned} \tag{14}$$

where s_{k+i} represents the error between the measured and estimated variables, and w_{k+i} is the state estimation error.

Therefore, at each instant of time k, knowing the vectors

$$U_k = \begin{bmatrix} u_{k-N} \\ u_{k-N+1} \\ \vdots \\ u_k \end{bmatrix} \in \mathbb{R}^m,\ Y_k = \begin{bmatrix} y_{k-N} \\ y_{k-N+1} \\ \vdots \\ y_k \end{bmatrix} \in \mathbb{R}^m, \tag{15}$$

and the initial state x_o, the constrained optimization problem

$$\begin{aligned} &\underset{\hat{X}_k}{\text{minimize}}\ \mathrm{J_k}(\hat{X}_k) \\ &\text{subject to } \hat{x}_{k+i+1} = \sum_{j=1}^{2^{r_d}} \mu_j(\vartheta_{k+i}) \left(A_{o_j} \hat{x}_{k+i} + B_{o_j} u_{k+i} \right) \\ &\qquad + w_{k+i} + E_d \Theta y_{k+i} \quad i = -N, \dots, 0 \\ &\qquad y_{k+i} = C_d \hat{x}_{k+i} + s_{k+i} \quad i = -N, \dots, 0 \\ &\qquad \hat{X}_k \in X_d, \end{aligned} \tag{16}$$

is solved online for

$$\hat{X}_k = \begin{bmatrix} \hat{x}_{k-N+1} \\ \hat{x}_{k-N+2} \\ \vdots \\ \hat{x}_{k+1} \end{bmatrix} \in \mathbb{R}^{n_x}, \tag{17}$$

where X_d is the constraint region for the dynamic states, n_x is the number of dynamic states, $Q = Q^T \geq 0$, $R = R^T > 0$, $P = P^T > 0$ and

$$\begin{aligned} A_{o_j} &= (I - E_d \Theta C_d) A_{d_j} \\ B_{o_j} &= (I - E_d \Theta C_d) B_{d_j}, \end{aligned}$$

are the unknown input matrices [26].

TABLE I
TS-MPC DESIGN PARAMETERS

Parameter	Value	Parameter	Value
Q	0.99*diag(0.66 0.01 0.33)	$\overline{u}$	[3.5 3]
R	0.01*diag(0.5 0.5)	$\underline{u}$	[0.1 -3]
T_c	0.05 s	$\overline{\Delta u}$	[0.3 0.3]
N	10	$\underline{\Delta u}$	[-0.3 -0.3]
R_{TS}	diag(1 3)	Q_{TS}	diag(1 1.5 3)

TABLE II
TS-MHE-UIO DESIGN PARAMETERS

Parameter	Value	Parameter	Value
Q	0.99*diag(0.33 0.33 0.33)	N	15
R	0.01*diag(0.5 0.5)	T_d	0.01 s
P	diag(2 2 2)	$\bar{\hat{x}}$	[3.5 2 3]
$\underline{\hat{x}}$	[0.1 -2 -3]		

TABLE III
TS-LQR DESIGN PARAMETERS

Parameter	Value
Q	0.99*diag(0.8 0.01 0.19)
R	0.01*diag(0.5 0.5)

V. SIMULATION RESULT

In this section, we validate the performance of the proposed control/observer scheme in a racing scenario through simulation in MATLAB.

The considered vehicle for running simulations is an scaled electric RWD one whose dynamics are presented in Appendix B. The conversion from acceleration and steering to their respective motor voltages is made by using a previously found map.

To show the effectiveness of the estimation scheme, we perform the comparison of adding the online estimated friction force to the TS-MPC control action (compensated in figures) against not estimating the friction force (no compensated in figures). As it is shown in Fig. 1, the current estimated friction force (F_{fr}) is converted in acceleration to be properly added to the control variable (a).

In addition, we show the promising results of the TS-MPC approach by performing a comparison against the non-linear MPC approach (NL-MPC in resulting figures).

The TS-MPC uses planning data to instanciate the state space matrices at every time step within the MPC prediction stage. To verify the real-time feasibility of the presented strategies, we perform the simulations on a DELL inspiron 15 (Intel core i7-8550U CPU @ 1.80 GHzx8).

Then, the optimal control problem (7) is solved at a frequency of 20 Hz using the solver GUROBI [27] through YALMIP [28] framework. For the non-linear MPC case, the solver IPOPT is used. This solves the position control problem in a outer loop (see Fig. 1). In the inner loop, the dynamic state feedback control problem (Section III-B) is solved at a rate of 200 Hz to control the velocities of the vehicle. The dynamic states used by this inner control law are provided by solving the optimal problem (16).

The vehicle model, TS-MPC, TS-MHE-UIO and dynamic TS-LQR parameters are listed in Tables V, I, II and III, respectively.

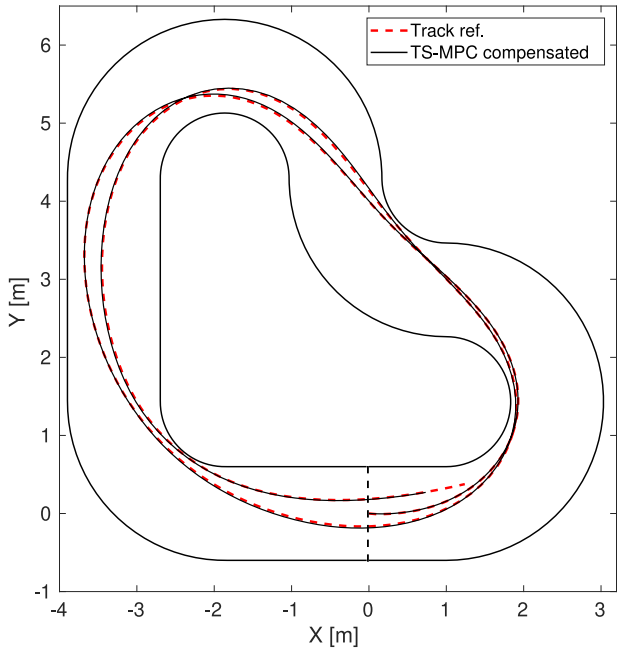

Fig. 3. Simulation circuit used for testing the proposed control technique.

Solving the problem (10) to determine the largest terminal set, we obtain matrix S as

$$S = \begin{bmatrix} 0.465 & 0 & 0 \\ 0 & 23.813 & 76.596 \\ 0 & 76.596 & 257.251 \end{bmatrix}. \quad (18)$$

The comparison is made in the circuit presented in Fig. 3. It is intended to show a racing situation in which the vehicle goes as fast as possible. For this, a reference obtained in an offline way is provided, which optimizes the trajectory by minimizing the lap time. In this way the automatic control of the vehicle becomes a greater challenge having to manage the behavior of the car very close to the dynamic limits of this. In addition, the vehicle performs under the influence of disturbance in the friction coefficient (see Fig. 4).

The friction force affecting the vehicle as well as the estimation of this by the TS-MHE-UIO are depicted in Fig. 4. It is seen how the observer is succesfully able to estimate the changing disturbance.

Below, in Fig. 5, we show both, the linear and angular speed profiles provided by the trajectory planning and the respective vehicle responses for every compared case. It can be appreciated a little better response in the linear velocity tracking by the NL-MPC approach, but also, by the TS-MPC algorithm with force compensation with respect to the non compensation scenario.

In Fig. 6, we illustrate the complete set of errors, i.e. position, orientation and velocities errors. It is seen the close behaviour between TS-MPC compensated and NL-MPC compensated. Moreover, it may be appreciated the effectivity of the compensation mechanism helping the controller to handle the coming external disturbances, and hence, helping to reduce the tracking errors.

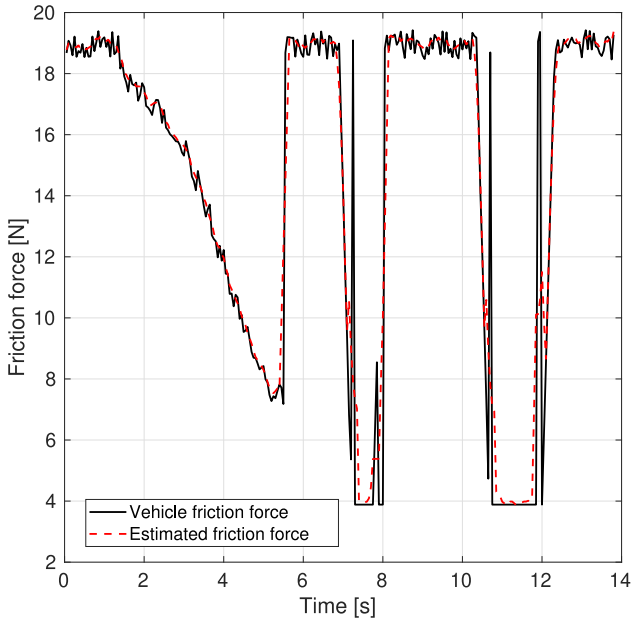

Fig. 4. Static friction force profile applied during the simulation test and the estimated friction force by the TS-MHE-UIO. This force is fixed on the vehicle longitudinal axle following the formula: $\mu(t)mg$, where $\mu(t)$ changes along the simulation.

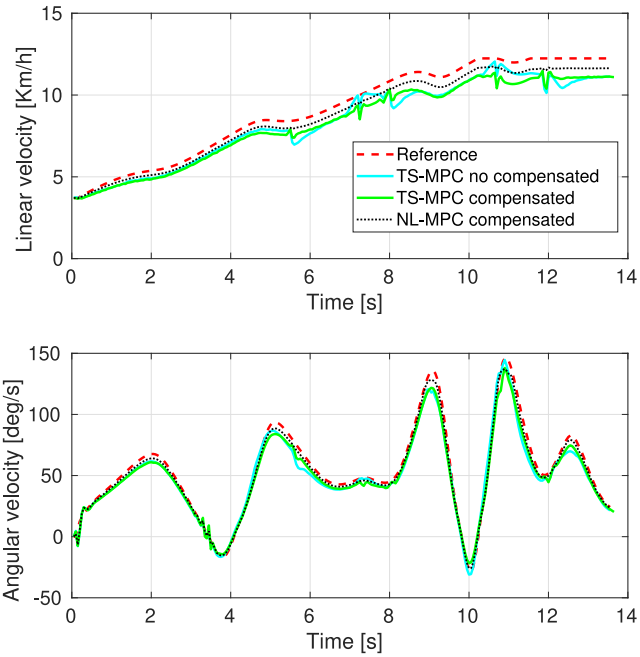

Fig. 5. Reference and response velocities for the three cases compared.

The respective control actions applied to the simulation vehicle are shown in Fig. 7. It is observed a similar response throughout the test even in the no compensated case. However, little differences in the actuation variables at high speeds may make the states response to be different.

An interesting aspect of racing behaviour as well as a good difficulty meter of the performance carried out is the slip angle on the wheels. The difference between the front slip angle

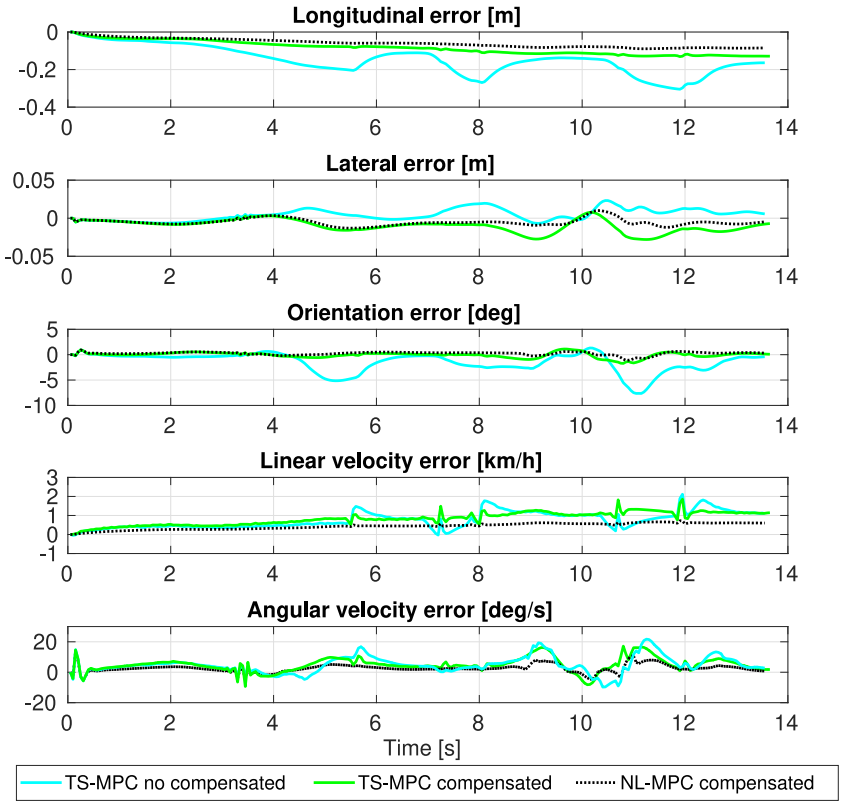

Fig. 6. Time evolution of the tracking errors for each compared kinematic control strategy.

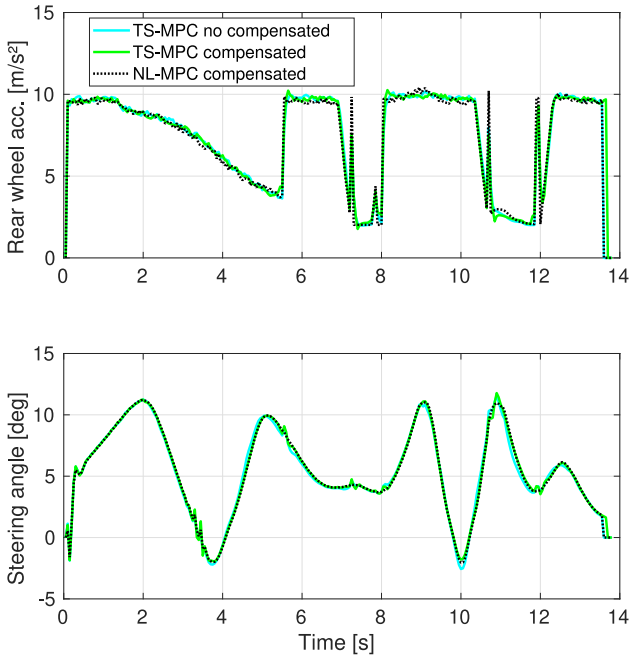

Fig. 7. Resulting control actions. Up: Linear acceleration applied over the rear wheel axle. Down: Steering angle applied on the front wheel.

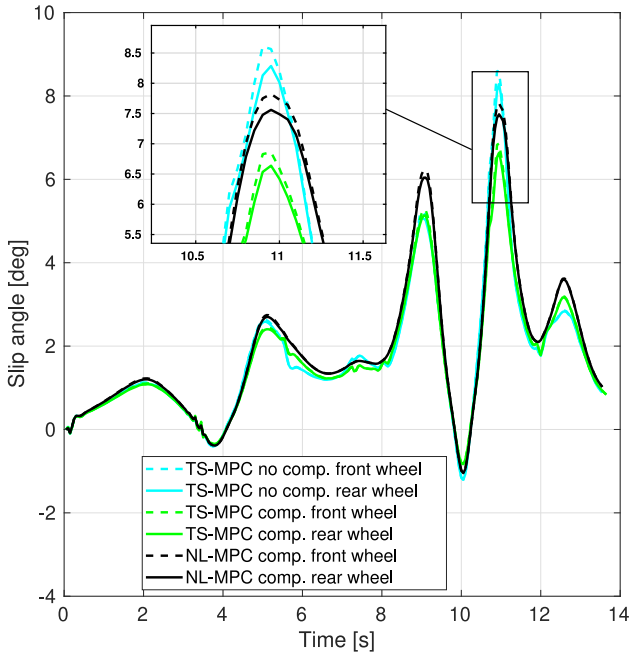

Fig. 8. Front and rear slip angles for the three compared cases.

and the rear slip angle gives us information about whether the vehicle enters the understeer or oversteer situation. In Fig. 8, it can be seen a set of large slip angles at the ending part of the simulation as well as some difference between the front and rear slip angles (see Fig. 8 zoom). The frontal slip angle situation greater than the rear slip angle is known as an understeer and is a behavior to avoid. In this case, we can appreciate

TABLE IV
COMPARISON USING A QUADRATIC MEASURE

Approach	$RMSE_x$	$RMSE_y$	$RMSE_\theta$	$RMSE_v$	$RMSE_w$
$TS\text{-}MPC\ no\ compensated$	0.167	0.015	0.042	0.240	0.131
$TS\text{-}MPC\ compensated$	0.091	0.013	0.009	0.241	0.116
$NL\text{-}MPC\ compensated$	0.063	0.008	0.007	0.129	0.063

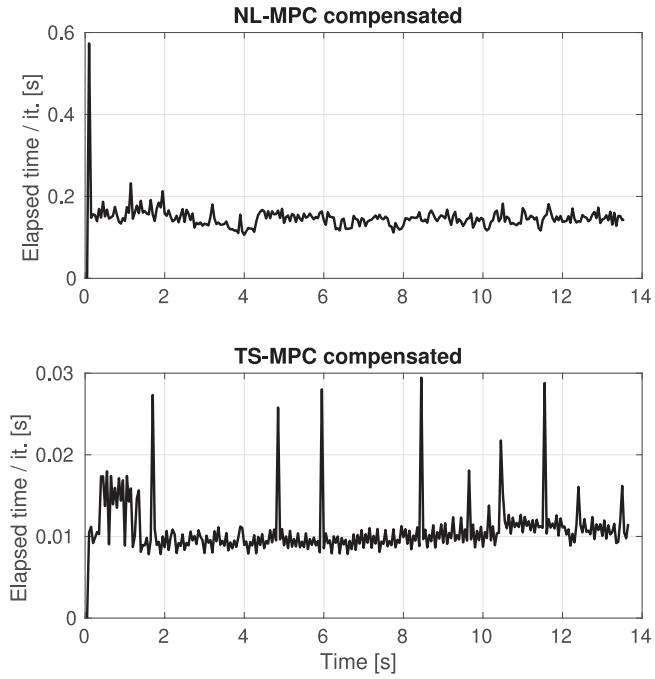

Fig. 9. Computational time when solving the kinematic MPC for both of the compensated cases.

this behavior due to a very fast and extreme driving in certain curves.

From a real time feasibility point of view, an aspect to highlight when dealing with control strategies based on optimization is the computational time spent at each optimization procedure. In Fig. 9 we show the elapsed time at each kinematic MPC optimization for the TS-MPC and NL-MPC approaches. It is shown the computational time improvement when using the TS-MPC strategy. Note that the non-linear optimization problem has been solved using IPOPT solver.

Finally, a quantitative comparison is made using the root mean squared error (RMSE) as performance measurement. It is shown in Table IV.

VI. CONCLUSION

In this work, a cascade control scheme (kinematic and dynamic) was presented to solve the problem of integrated control (lateral and longitudinal) of autonomous vehicles.

The novel kinematic control was designed using the Model Predictive Control technique with the prediction model expressed in the Takagi Sugeno formulation (TS-MPC) without using any linearisation. On the other hand, the dynamic control was approached using the Linear Quadratic Regulator strategy, with a Takagi Sugeno modeling and using a LMI formulation of the problem (TS-LMI-LQR).

A comparison was made between two methods of solving the control problem: using the non-linear MPC formulation (NL-MPC) and using the TS-MPC approach being the TS model instanciated at each prediction step within the prediction stage using planning data. It was demonstrated that the TS-MPC technique presents a close performance to the non-linear control problem but in a much faster way (between 10 and 20 times).

In addition, a Takagi Sugeno - Moving Horizon Estimator - Unknown Input Observer (TS-MHE-UIO) was introduced with the aim of estimating dynamic states and disturbances acting on the vehicle, such as the friction force. The estimation of the friction force is used to compensate the disturbance and allow lower control efforts. It was also demonstrated the effectiveness of this mechanism in the comparison performed.

As future research, it is planned to apply the proposed strategy in a real vehicle.

APPENDIX A
VEHICLE MODEL FOR CONTROL

The non-linear equations employed for control purposes are presented as

$$
\begin{aligned}
\dot{x}_e &= \omega y_e + v_d \cos\theta_e - v_x \\
\dot{y}_e &= -\omega x_e + v_d \sin\theta_e \\
\dot{\theta}_e &= \omega_d - \omega \\
\dot{v}_x &= a - \frac{F_{yF}\sin\delta}{m} - \frac{F_f}{m} + \omega v_y \\
\dot{v}_y &= \frac{F_{yF}\cos\delta}{m} + \frac{F_{yR}}{m} - \omega v_x \\
\dot{\omega} &= \frac{F_{yF} l_f \cos\delta - F_{yR} l_r}{I} \\
F_{yF} &= C_x\left(\delta - \frac{v_y}{v_x} - \frac{l_f\omega}{v_x}\right) \\
F_{yR} &= C_x\left(-\frac{v_y}{v_x} + \frac{l_r\omega}{v_x}\right) \\
F_f &= \mu_o m g
\end{aligned}
\tag{19}
$$

Refer to the Appendix A in [25] for the complete development of the position error model.

TABLE V
DYNAMIC MODEL PARAMETERS

Parameter	Value	Parameter	Value
l_f	$0.125\ m$	l_r	$0.125\ m$
m	$1.98\ kg$	I	$0.03\ kg\ m^2$
C_f	$68\ \frac{N}{rad}$	C_r	$71\ \frac{N}{rad}$
d	9.72	c	1.3
b	6.1	μ_o	0.95
κ	0.05		

APPENDIX B
VEHICLE MODEL FOR SIMULATION

For simulation purposes we use a higher fidelity vehicle model. Unlike the model used for control design, this considers a more precise tire model, i.e. the Pacejka "Magic Formula" tire model where the parameters b, c and d define the shape of the semi-empirical curve. Parameter κ represents the aerodynamic drag coefficient. Also, a more accurate computation of the tire slip angles is given.

$$
\begin{aligned}
\dot{x} &= \cos\theta v_x - \sin\theta v_y \\
\dot{y} &= \sin\theta v_x + \cos\theta v_y \\
\dot{\theta} &= \omega \\
\dot{v}_x &= a - \frac{F_{yF}\sin\delta}{m} - \frac{F_{df}}{m} + \omega v_y \\
\dot{v}_y &= \frac{F_{yF}\cos\delta}{m} + \frac{F_{yR}}{m} - \omega v_x \\
\dot{\omega} &= \frac{F_{yF} l_f \cos\delta - F_{yR} l_r}{I} \\
F_{yF} &= d\sin\left(c\tan^{-1}(b\alpha_f)\right) \\
F_{yR} &= d\sin\left(c\tan^{-1}(b\alpha_r)\right) \\
\alpha_f &= \delta - \tan^{-1}\left(\frac{v_y}{v_x} + \frac{l_f\omega}{v_x}\right) \\
\alpha_r &= -\tan^{-1}\left(\frac{v_y}{v_x} - \frac{l_r\omega}{v_x}\right) \\
F_{df} &= \mu m g + \kappa v_x^2
\end{aligned}
\tag{20}
$$

All parameters are properly defined in Table V.

REFERENCES

[1] J. Jiang and A. Astolfi, "Lateral control of an autonomous vehicle," *IEEE Trans. Intell. Vehicles*, vol. 3, no. 2, pp. 228–237, Jun. 2018.

[2] J. Yang, H. Bao, N. Ma, and Z. Xuan, "An algorithm of curved path tracking with prediction model for autonomous vehicle," in *Proc. 13th Int. Conf. Comput. Intell. Secur.*, 2017, pp. 405–408.

[3] A. Boyali, S. Mita, and V. John, "A tutorial on autonomous vehicle steering controller design, simulation, and implementation," arXiv:1803.03758, 2018.

[4] H. M. Y. Naeem and A. Mahmood, "Autonomous cruise control of car using lqr and h2 control algorithm," in *Proc. Int. Conf. Intell. Syst. Eng.*, 2016, pp. 123–128.

[5] K. M. Junaid, W. Shuning, K. Usman, and R. Naveed, "LQR autonomous longitudinal cruise control with a minimum order state observer," in *Proc. 8th IASTED Int. Conf.*, Cambridge, USA, vol. 31, 2005.

[6] K. Tanaka and H. O. Wang, *Fuzzy Control Systems Design and Analysis: A Linear Matrix Inequality Approach*. Hoboken, NJ, USA: Wiley, 2004.

[7] P. Gáspár, Z. Szabó, J. Bokor, and B. Németh, *Robust Control Design for Active Driver Assistance Systems.* New York, NY, USA: Springer, 2016.

[8] D. Rotondo, *Advances in Gain-Scheduling and Fault Tolerant Control Techniques*. New York, NY, USA: Springer, 2017.

[9] E. Ostertag, *Mono-and Multivariable Control and Estimation: Linear, Quadratic, and LMI Methods*. Berlin, Germany: Springer Science & Business Media, 2011.

[10] G.-R. Duan and H.-H. Yu, *LMIs in Control Systems: Analysis, Design and Applications*. Boca Raton, FL, USA: CRC press, 2013.

[11] S. Blažič, "Two approaches for nonlinear control of wheeled mobile robots," in *Proc. 13th IEEE Int. Conf. Control Autom.*, 2017, pp. 946–951.

[12] J. B. Rawlings and M. J. Risbeck, "Model predictive control with discrete actuators: Theory and application," *Automatica*, vol. 78, pp. 258–265, 2017.

[13] J.-P. Corriou, "Model predictive control," in *Process Control*. New York, NY, USA: Springer, 2018, pp. 631–677.

[14] D. Q. Mayne, "Model predictive control: Recent developments and future promise," *Automatica*, vol. 50, no. 12, pp. 2967–2986, 2014.

[15] Z. Ercan, M. Gokasan, and F. Borrelli, "An adaptive and predictive controller design for lateral control of an autonomous vehicle," in *Proc. IEEE Int. Conf. Veh. Electron. Saf.*, 2017, pp. 13–18.

[16] Y. Xu, B. Chen, X. Shan, W. Jia, Z. Lu, and G. Xu, "Model predictive control for lane keeping system in autonomous vehicle," in *Proc. 7th Int. Conf. Power Electron. Syst. Appl.-Smart Mobility, Power Transfer Secur.*, 2017, pp. 1–5.

[17] P. S. Cisneros, S. Voss, and H. Werner, "Efficient nonlinear model predictive control via quasi-lpv representation," in *Proc. IEEE 55th Conf. Decis. Control*, 2016, pp. 3216–3221.

[18] T. Besselmann and M. Morari, "Autonomous vehicle steering using explicit LPV-MPC," in *Proc. Eur. Control Conf.*, 2009, pp. 2628–2633.

[19] O. Sename, P. Gaspar, and J. Bokor, *Robust Control and Linear Parameter Varying Approaches: Application to Vehicle Dynamics*. New York, NY, USA: Springer, 2013, vol. 437.

[20] K. Yi, K. Hedrick, and S.-C. Lee, "Estimation of tire-road friction using observer based identifiers," *Vehicle Syst. Dyn.*, vol. 31, no. 4, pp. 233–261, 1999.

[21] J. Svendenius, "Tire modeling and friction estimation," Ph.D. dissertation, Dept. Autom. Control, Lund Inst. Technol., Lund Univ., Lund, Sweden, 2007.

[22] J. Dakhlallah, S. Glaser, S. Mammar, and Y. Sebsadji, "Tire-road forces estimation using extended Kalman filter and sideslip angle evaluation," in *Proc. Amer. Control Conf.*, 2008, pp. 4597–4602.

[23] E. Alcala, V. Puig, J. Quevedo, and T. Escobet, "Gain scheduling LPV control for autonomous vehicles including friction force estimation and compensation mechanism," *IET Control Theory Appl.*, vol. 12, pp. 1683–1693, 2018.

[24] A. Amrane, A. Larabi, and A. Aitouche, "Actuator fault estimation based on LPV unknown input observer for induction machine," *Stud. Informat. Control*, vol. 26, no. 3, pp. 295–304, 2017.

[25] E. Alcala, V. Puig, J. Quevedo, T. Escobet, and R. Comasolivas, "Autonomous vehicle control using a kinematic Lyapunov-based technique with LQR-LMI tuning," *Control Eng. Pract.*, vol. 73, pp. 1–12, 2018.

[26] J. Keller and M. Darouach, "Two-stage Kalman estimator with unknown exogenous inputs," *Automatica*, vol. 35, no. 2, pp. 339–342, 1999.

[27] G. Optimization, Inc.,"Gurobi optimizer reference manual," 2015," Google Scholar, 2014.

[28] J. Lofberg, "Yalmip: A toolbox for modeling and optimization in MATLAB," in *Proc. IEEE Int. Symp. Comput. Aided Control Syst. Des.*, 2004, pp. 284–289.

Eugenio Alcalá was born in Spain in 1992. He received the bachelor's degree in electronics and automation from Universidad de Zaragoza, Teruel, Spain, in 2014, and the robotics and control master's degree from Universitat Politcnica de Catalunya, Barcelona, Spain, in 2016. He is currently working toward the Ph.D. thesis within the automatic control field applied on autonomous vehicles. He is on the Advanced Control Systems (SAC) Research Group, Research Center for Supervision, Safety, and Automatic Control (CS2AC), UPC. His main research interests include linear parameter varying based, optimal and robust control applied to solve new autonomous driving problems.

Vicenç Puig was born in Spain in 1969. He received the Ph.D. degree in control engineering in 1999 and the telecommunications engineering degree in 1993, both from Universitat Politcnica de Catalunya, Barcelona, Spain. He is currently a Full Professor of automatic control and the Leader of the Advanced Control Systems Research Group, Research Center for Supervision, Safety, and Automatic Control, UPC. His main research interests include fault detection, isolation, and fault-tolerant control of dynamic systems. He has been involved in several European projects and networks, and has published many papers in international conference proceedings and scientific journals.

Joseba Quevedo is currently a Professor at the Polytechnic University of Catalonia, Barcelona, Spain, in automatic control domain, where he has been a Full Professor since 1991. He has published more than 400 articles in scientific journals and congresses in the areas of advanced control, identification, and estimation of parameters, detection, and diagnosis of faults, fault-tolerant control and their applications in large-scale systems (systems water distribution and sewage networks), and industrial processes. He has participated in many Spanish and European Research Projects in the field of advanced control and supervision and its application in complex systems. Since 2014, he has been the Director of the CS2AC UPC Research Center (Supervision Center and Security and Automatic Control) with more than 30 researchers, and from 2014 to 2018 he was the President of the Spanish Committee of Automatic Control with more than 300 Automation and Robotics specialists from Spain.